

---

# Normal Versus Malignant Cell Classification in B-allwhite Blood Cancer Microscopic Images Using Deep Learning

Asad Ullah<sup>1</sup>, Muhammad Shoaib<sup>2,\*</sup>

<sup>1</sup>Department of Computer Science and Technology, Abasyn University, Peshawar, Pakistan

<sup>2</sup>Department of Computer Science, CECOS University of IT and Emerging Sciences, Peshawar, Pakistan

## Email address:

shoaib1646@gmail.com (Muhammad Shoaib)

\*Corresponding author

## To cite this article:

Asad Ullah, Muhammad Shoaib. Normal Versus Malignant Cell Classification in B-allwhite Blood Cancer Microscopic Images Using Deep Learning. *American Journal of Computer Science and Technology*. Vol. 5, No. 3, 2022, pp. 190-197. doi: 10.11648/j.ajcst.20220503.16

**Received:** July 12, 2022; **Accepted:** August 4, 2022; **Published:** September 29, 2022

---

**Abstract:** In diagnosing cancer and determining its progress, an important aspect is the identification of malignant cells. Blood diseases such as leukemia are generally detected when cancer cells are much larger than normal cells in the late stages. Due to strong morphological similarities, the differentiation of cancer cells from normal blood cells is a challenge. Compared with normal cells, the precise classification of malignant cells in a microscopic image of blood cells depends on the early diagnosis of leukaemia. Transfer learning and fine-tuning of the VGG16 convolutional neural network through batch normalization can resolve the malignant and normal white blood cells classification problem with higher accuracy. Applying CLAHE to enhance image data quality is then passed as input to the network for training purposes. The results acquired by the fine-tuning of triple-loss and cross-entropy or cross-entropy loss with L2 normalization are compared. Furthermore, fine-tuning on a combined training validation dataset using simple cross-entropy loss can improve the model's performance. As an effective technique for diagnosing leukaemia, computer-aided cell classification has become popular. Fine-tuning VGG16 neural networks to classify normal and malignant cell images through batch standardization is part of our classification method. The proposed convolutional neural network detects cancer and normal cells with greater accuracy and time efficiency.

**Keywords:** Microscopic Images, Leukemia, Computer Aided Diagnosis, Deep Learning

---

## 1. Introduction

Continuous development of cancer research has been carried out over the past few decades. Scientists have used various methods to detect the type of cancer before it causes symptoms, such as early screening [1]. Also, at an early stage, they have developed new strategies for Cancer Prediction outcomes. Many cancer data has been collected for use by the medical research community with ad-new medical technology. However, precise Disease prediction outcomes it is one of the most exciting and challenging tasks for physicians. For medical researchers, machine learning has become a popular tool as a result [2]. These methods can identify and identify patterns from complex data sets and their relationships while effectively predicting future cancer types.

Given the importance of personalized medicine and the

growing ML technology application trend, we review the research using this cancer prediction and progress techniques [3]. In these studies, cancer patients' prognostic and predictive characteristics were considered independent of specific therapies or integrated into guided treatments. We'll also discuss the types of ML technologies used, the types of information they combine, and the overall performance of each proposed scenario, as well as their advantages and disadvantages.

In the proposed work, notable trends include integrating mixed data, such as clinical and genomic data. However, the lack of external validation or testing of predictive model performance is a common issue we have noticed in several books. The ML method application can improve the susceptibility to cancer, recurrence rate, and the accuracy of prediction of survival. The accuracy of cancer prediction outcomes has significantly improved by 15 percent to 20 percent in recent years using ML technology [4].

Several studies based on different strategies to achieve early cancer diagnosis and prognosis have been reported in the literature. Specifically, these studies describe cyclic miRNA spectrometry related methods that have proven to be a good cancer detection and identification category [5]. However, in early screening, these techniques are less sensitive to use and difficult to distinguish between benign and malignant tumors. Various elements are discussed in the prediction of cancer outcomes based on gene expression characteristics. In predicting cancer outcomes, these studies list the potential and limitations of microarrays. Although genetic markers Our prognosis in cancer patients can significantly improve, not enough progress has been made clinically. However, data samples need to be studied more extensively and thoroughly validated Before expression of genes spectrum analysis In clinical practice, it can be used.

Leukemia is a type of blood cancer that starts in the bone marrow and leads to abnormal blood cell production [6]. Such WBC cells nucleus are destroyed and are also known as exploded cells. There are variations in the causes of suspected leukemia. High-risk variables include genetic and environmental factors, smoking, prolonged exposure to ionizing radiation, benzene, chemotherapy and Down syndrome. Acute lymphoblastic leukemia (ALL), acute myeloid leukemia (AML), chronic lymphoblastic leukemia (CLL), and chronic myeloid leukemia (CML) are four types of blood cancer [7]. To detect blood cancer, a blood sample or bone marrow using a biopsy procedure is examined by a histopathologist to detect blood cancer. In the late stages of blood diseases, such as leukemia the number of abnormal (Malignant) blood cancers is equal to or higher than normal cells. The manual classification of malignant and normal cells by pathologists is critical to diagnose these blood diseases early. Computer-vision and machine learning aided based leukemia diagnostic systems have attracted great interest as an early cancer diagnosis method. Cells have been classified through computer vision to diagnose leukemia and determine its stage and type. Artificial intelligence-based cancer cell recognition is a very accurate, efficient, and easy-to-use method [8].

However, distinguishing between cancer and normal white blood cells can be challenging due to the morphological similarity. This research article structure is as follows:

Literature review cancer cells classification is discussed in section 2. Our proposed model for cancer and normal cell classification is covered in section 3. In Section 4, the experimental result acquired from the proposed model is visualized and discussed.

## 2. Literature Review

The best choice for medical imaging applications such as detection and classification is currently deep learning using convolutional neural networks (CNN). Although CNN achieves the best results on large data sets, training requires many data and computing resources. The data set is limited in many instances and may not be sufficient to train CNN from the

outset. Transfer learning can be used in this situation to take advantage of the capabilities of CNN while reducing the cost of computing. In this strategy, CNN initially pre-trained and then applied it to specific tasks on a large and diverse standard image dataset. Several pre-trained neural networks, such as VGGNet, Resnet, Nasnet, Mobilenet, Inception, and Xception15, have won international competitions [9]. In evaluating different CNN architectures, transfer learning scored highest in the classification of lymph nodes (LN) and interstitial pulmonary disease (ILD) in the chest and abdomen.

To distinguish malignant cells from non-malignant cells, the authors used an average combined classification because using a pre-trained CNN architecture fed into a fully connected classification layer; they extracted features from breast cancer images. [3]. The experimental results show that their model is more accurate than all other CNN methods to classify and classify breast tumors based on cell images. Further work is based on a range of deep learning architectures to improve transfer learning usefulness for cell-based image classification. In transfer learning, it is used in cytological images on previously published standard baseline data sets to overcome breast cancer detection models' limitations [10].

These approaches have in common that many of the pre-trained CNN model features are used (up to 100upK). Since many of these features are redundant or contain zeros, they are inefficient in time and computing resources. Furthermore, the classifier's accuracy can benefit from limiting the number of features. In previous work, white blood cell detection was performed using classical image processing by extracting various features (including colours, textures, shapes, blending features) and then using social spider-inspired optimization methods to select the most useful features [11]. In ALL-IDB2, the same data set as this work, the model was tested. The accuracy, sensitivity, and specificity of the split outcomes were 99.2%, 100%, and 97.1%, respectively, and the model classification accuracy was by far the best published [12].

To distinguish between ALL and AML subtypes in leukaemia datasets, Super Neural Network (FHSNN) fuzzy classifier is offered. Since the number of genes exceeds the number of samples available in the DNA chip dataset [13], pre-trained dimensional reduction techniques such as signal-to-noise ratio (SNR), spacing, rank, and Wilcoxon statistics, and reporting by Fisher is subject to the data set [14]. Experimental results show that, with fewer genes than previously published methods, FHSNN can achieve 100 percent accuracy [15]. A new algorithm for artificial neural networks (ANN) was introduced by Adjouadi [16] to improve the classification of multidimensional data, highlighting the classification of abnormal blood samples relative to normal blood samples (i.e., AML and LAL). All ratings achieve an accuracy of 96.67 percent through this algorithm.

An amendment to FHSNN, an improved ultra-fuzzy neural network, to differentiate between LAL and AML in

the Leukemia Data Set was proposed by Fabio Scotti, Department of Information Technology, University of Milan (Università degli Studi di Milano) [17]. Using dimension-reducing techniques such as the Spaceman correlation coefficient and Wilcoxon rank, gene selection is carried out. With only two genes, using the MFHSNN classifier, 100 percent classification precision can be obtained. The proposed model is a novel method of how acute lymphoblastic leukemia cells and normal cells can be distinguished [18]. The k-average algorithm is classified as the cell's nucleation after pre- image processing of microscopic blood cell images. Geometric and statistical features are extracted from the cell's nucleation to be classified through the use of a support vector machine. To process datasets, all of these methods use dimension reduction or special network structures. Our system uses a network of reeling neurons with common weights. In addition, our strategy reduces the time required. it takes to form a network compared to normal cell classification by starting with a pre-formed network and recycling it into leukemia mother cells.

### 3. Methodology

The transfer learning approach is adopted in the VGG16 CNN model pre-trained initially with ImageNet 1000 classes

dataset; the same model is modified by replacing the last two layers, i.e., softmax and classification output layers, along with fully connected layer with two output nodes. The modified network is trained with the custom malignant and normal cell images for developing an automatic cancer cells detection system.

### 4. VGG16

VGG16 is a convolutional neural network architecture (CNN) developed to rival the ImageNet Wide-Area Optical Recognition.

Challenge by the Oxford Visual Engineering Group (ILSVRC). The ImageNet is a benchmark dataset consisting of 14 million images spread across 1,000 different categories of objects. The VGG16 CNN model won the ILSVRC challenge, which happens back in 2014, by achieving the highest accuracy for classifying 1000 class images among the competitors' models.

The network has a sophisticated design that utilizes various 3 x 3 filters and is stacked to form a normalization layer on top of each other. Such a stack of layers helps in capturing more information with a lower amount of computing. A feature map resulting from three remnants stacked with 3 x 3 filters has less computational overload and maybe equivalent to a single 7 x 7 filter smoothing layer.

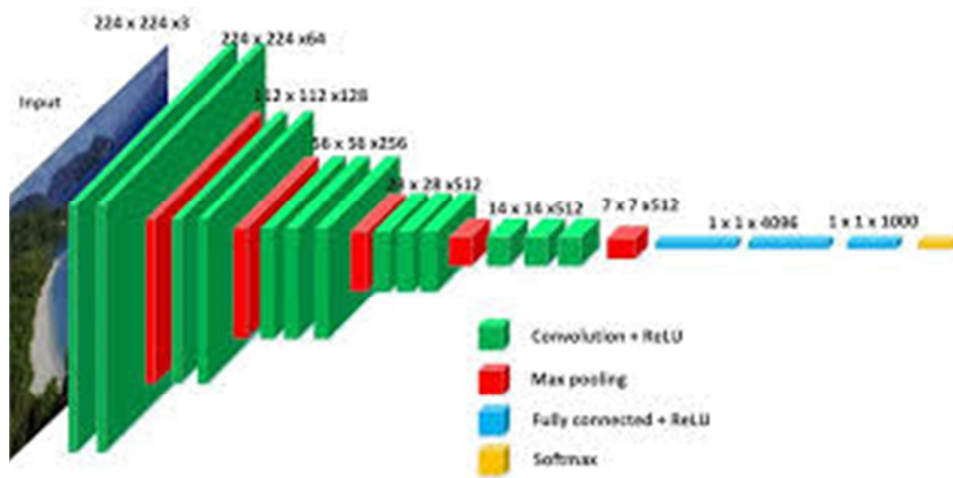


Figure 1. Architecture of VGG16.

The maximum pooled layer consists of 2 x 2 filter that reduces input by two times as much as the maximum value near output 2 x 2. The input image to the VGG16 model is reduced four times its original size. The grid ends with two fully connected layers where each layer has 4,096 input nodes and 1,000 output nodes followed by a softmax and classification output layer. A fully connected layer associates each layer node with each feature element in the input. These fully connected layers restrict network input to fixed input size of 224 x 224 x 3. A softmax classifier uses  $\sigma$  that applies softmax (the data) to a fully connected layer's output characteristics.

$$\alpha(z)_j = e^{z_j} / \sum_k e^{z_k}$$

For  $j = 1, \dots, k$

and

$$Z1 = (z_1, \dots, z_1)$$

The maximum pooled layer is made up of 2 x 2 cores that decrease the input by two times the maximum value of 2 x 2 near the output. The entry size is reduced to 4 times the minimum. The grid ends with two fully linked layers, each containing 4,096 sections, followed by 1,000 Softmax classifier sections. With a fully connected layer, each layer

node is associated with each feature element in the input. These fully linked layers limit network input to a  $224 \times 224 \times 3$  fixed size. A softmax classifier is a full  $\sigma$  that applies

softmax (the data) to a fully connected layer's output characteristics.

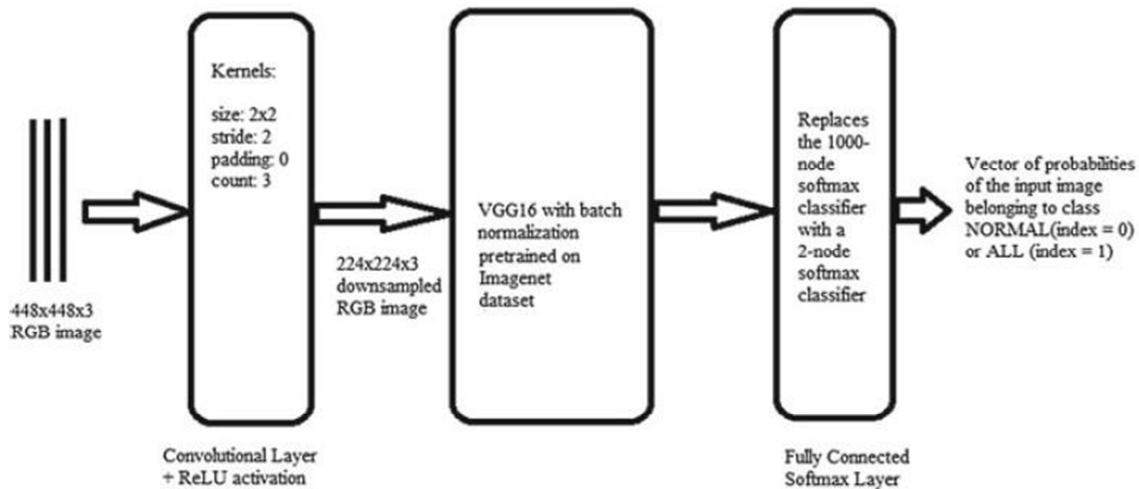


Figure 2. These fully linked layers limit network input to a  $224 \times 224 \times 3$  fixed size.

## 5. Batch Normalization

Typically, neural networks consist of a small number of input batches and are sampled from more extensive datasets. The distribution of the entry batch's median value, however, varies from batch to batch. Deformation"deformation" The behavior of neural networks is affected by changes in the input data distribution. Neural networks are trained to alter each layer's weight, thus altering its activation process. The output distribution of each layer changes as formations advance, forcing the next layer to adapt to these modifications. The conversion of variables extends the time needed to form the network's middle layer.

Bulk adjustment is used to standardize the activation process, with an average output of 0 unit variance per weighted layer. This stabilizes the input speed to the next layer and accelerates the formation. The limitation of these activations to values between 1 and -1 can, however, compromise learning. As a result, the batch smoothing layer can learn to adjust the  $\gamma$  parameters and extend and convert natural activations. Bulk standardization can also improve the performance of networks. VGG16 has a higher error rate than the simplified batch standardization of 26.63%. The highest error rate for VGG16 is 28.41%. For the correct category of the input image, the first

error rate measures the prediction error.

## 6. Transfer Learning

It is a complex and time consuming process to train a CNN with certain random hyper-parameters on a large image dataset. The transfer learning approach can be followed by removing the old learning from an existing CNN model instead of developing a new CNN model that is a tedious and challenging task and training the same model with some custom datasets by employing few model changes. In transfer learning, fine-tuning is carried out which updates all model parameters to suit the new dataset. The previously tested VGG16 network on a large ImageNet dataset demonstrates transfer learning to extend it to images outside the ImageNet dataset. To detect malignant white blood cells compared with normal blood cells, transfer learning in the VGG16 network is therefore carried out.

### 6.1. Data

The training and test data set presented consists of microscopic photos of two categories of cells: ALL (Malignant) and NORMAL. From several subjects with different identifiers, information from both classes is obtained. See Table 1 for configuring datasets.

Table 1. Composition of datasets.

Dataset	ALL Images	ALL Subjects	Normal Images	Normal Subjects
Training	7270	48	3390	29

### 6.2. Data Preprocessing

3-channel images in the format of  $450 \times 450$  are unique microscopic photos. To remove lighting differences, use point standardization to pre-process images.

Acquisition and pre-processing of data are described in 9-13 in more detail. Normal data is added to equalize the number of pictures of both types by applying horizontal and vertical inverse and 90, 180, and 270-degree rotation combinations. Just  $224 \times 224 \times 3$  input channels are accepted by the VGG16 architecture. You have to keep the photo of

the input microscope to a minimum before entering the grid. The image is 450 x 450 in size and is cropped to 448 x 448 images in the centre for capture. There is little chance that information will be lost because these images' limitations are part of the background. To scale the picture twice, use the network pre-layer converted by VGG16. To improve contrast and fine detail (see Figure 3) before inserting the mesh, apply the completed adaptive contrast histogram equation (CLAHE) to all images. The image is displayed in the YUV color space, whereas CLAHE is generated only on the Y channel. In the RGB color space, the image is then displayed again.

### 6.3. Finetuning

With a batch standardization layer, the network has the same

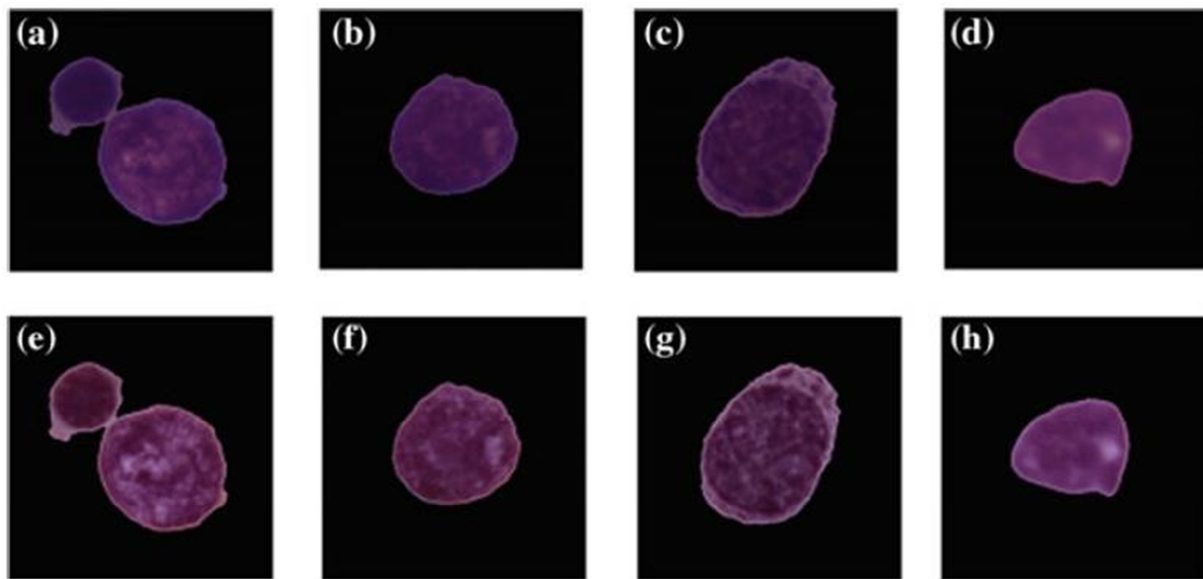


**Figure 3.** Images a and d are Malignant White blood cell images whereas the image e and h are the enhanced images of a and d images. Similarly, image b and c are Normal WBCs whose enhanced images can be seen in f and g.

### 6.4. Observations

The training dataset (5 images per class) is divided into ten batches. These batches are then passed to the CNN for model training. The total number of batches are 1455, and the size of the dataset is 14,550. Each batch of images also needs to be flipped horizontally and vertically, with a 0.5 probability of rotating 90, 180, and 270 degrees per conversion.

### 6.5. Stage 1 Training Cross-Entropy Loss

A classification model's performance can be measured using Entropy loss that produces probability values between 0 and 1 for each category. The only encoded label vector is the model target, the 0 and 1 label vectors that correspond to the actual entry category. The order of losses varies, depending on the expected probability of the category and its target name. For example, for a category where the target specifies one as an

pre-driven VGG16 standard network architecture. Add three layers of 2 x 2 cores and a reLU-enabled relu layer to the second sample input image network at 448 x 448 resolution.

This layer's output consists of three 224 x 224 channels connected to the original network of VGG16. This course provides the advantages of learning shorthand through training. The final softmax network layer was reconfigured to contain only two NORMAL (0), and ALL (1) input data outputs corresponding to each category, respectively (see Figure 2).

In phases, training was conducted. Only the training data is recycled from the network in the first phase, and the initial test dataset is used for validation. In the Phase 2 validation package, the model is also optimized to enhance performance.

essential loss value, the predicted probability is 0.1.

$$\text{Cross Entropy Loss (p, y)} = -\sum_i y_i \log(p_i)$$

$$\text{For } i = 1, \dots, K$$

where p is the probability vector corresponding to class K and the unique encoded label vector. Loss on average per payment. The network is formed by the loss of two types of cross-entropy. A random gradient drop with a usage time of 0.9 optimizes loss. Set the learning rate to 0.01 until the 10th time divided by twice every two periods, and then halved every ten cycles. However, in the first 10 to 15 periods, the validation set's best performance was obtained.

As shown in Figure 4, network loss can be optimized by implementing CLAHE. Also, as shown in Figure 5, we get better performance in the CLAHE verification package.

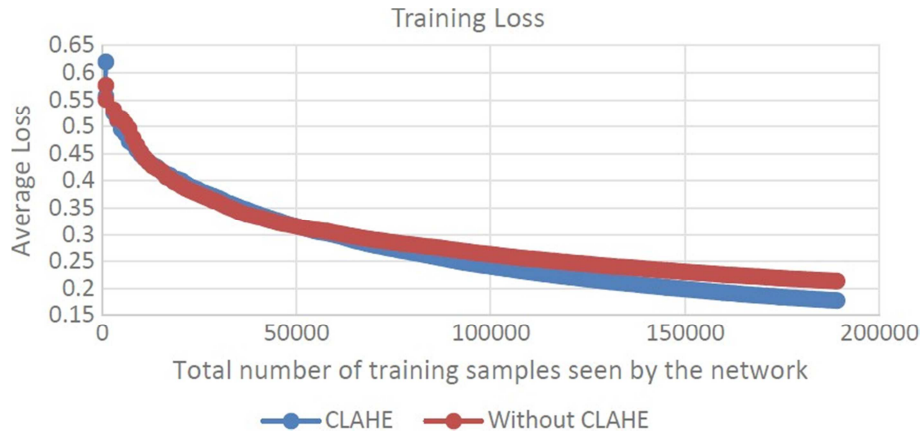


**Figure 4.** The average training loss seen by the network is compared to the total number of training samples (i) using CLAHE input and (ii) not using CLAHE input. The images used for model training are not unique because the dataset images are used once per epoch. The parameters set for CLAHE are: limit of the clip is 2.0 and grid size  $s \times 8$ .

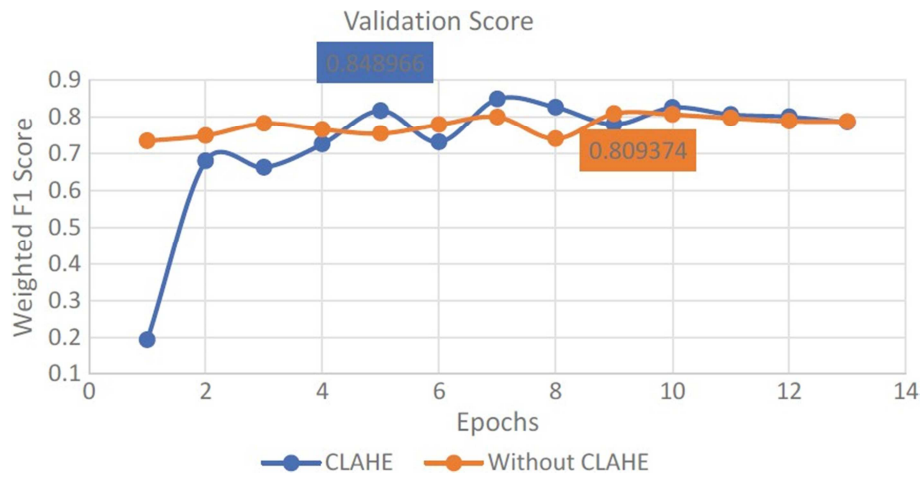


**Figure 5.** Validation score of training samples.

### 6.6. Stage 2 Training

For better output on the test's final dataset, the best performing model on the validation set (weighted F1 score of 0.848966) is further optimized. The hyper-parameter such as the number of epochs, Batchsize, optimizer etc. are fine-tuned for the cell image training and validation set. L2 normalization (the normalization coefficient is 0.001) and a combination of cross-entropy which are also standard hyper-parameters used for practical model training.

#### Triplet Loss

The three-state loss method is used to calculate the similarity between three-state samples. Batches include baseline samples (anchor points,  $a$ ), positive samples ( $p$ ) and negative samples ( $n$ ). As the resemblance between  $a$  and  $p$  decreases or the resemblance between  $a$  and  $n$  rises, the loss value increases. Its euclidean distance usually measures similarity.

$$L(a, p, n) = \max\{d(a_i, p_i) - d(a_i, n_i) + \text{margin}, 0\}$$

$$\text{For } i = 1, \dots, K$$

where  $d(x, y) = \|x - y\|_2$  is the Euclidean distance between  $x$  and  $y$  and  $K$  is the number of triples in the batch. Using a triple-state loss training network ensures that the characteristics of the network-generated anchor and positive samples are close together, while the characteristics of the negative sample are at least as far apart from the anchor's features positive samples. The features computed using the trained network are easily grouped into classes that can be easily separated using a margin value.

The combination of triple-state loss and cross-entropy loss was tried as a hypermeter for the model training. Three-state loss (before the softmax function is applied) is calculated from batches of 10 feature vectors calculated from the network in ten three-groups. For example, for each feature vector used as an anchor, select the same sample class's feature vector at the maximum Euthio mile distance from the anchor. Select a feature vector for a different sample type with the smallest distance from the anchor point as a negative example. Although L2 normalization optimizes losses better than other methods (see Figure 6), the initial test dataset performs best when training the composite dataset network (see Figure 7).



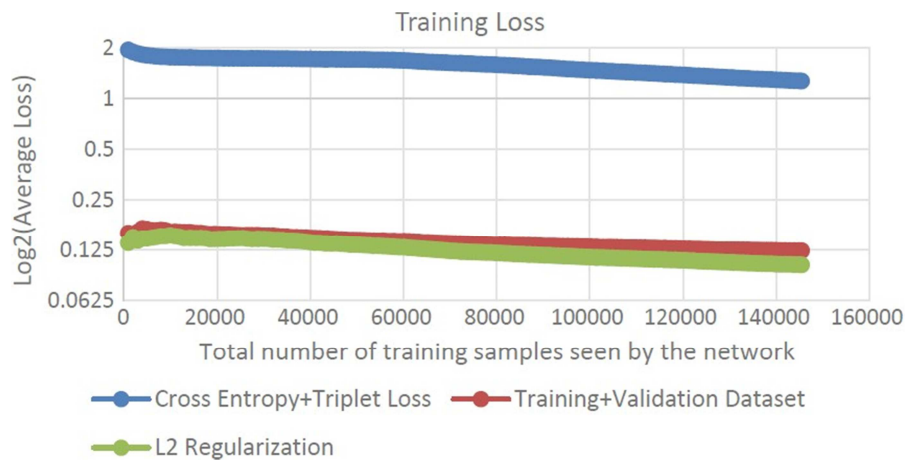


**Figure 6.** The average training loss is the sum of the total number of training samples seen by the network (i) the cross-entropy loss for training and testing dataset (ii) L2 normalization ( $\lambda = 0.001$ ) with cross-entropy loss and (iii) cross entropy loss with triplet loss. The images used for model training are not unique because they are used once per epoch in the dataset. Fine-tuning was performed on the combination of training and validation datasets used in Phase 1 of the network.

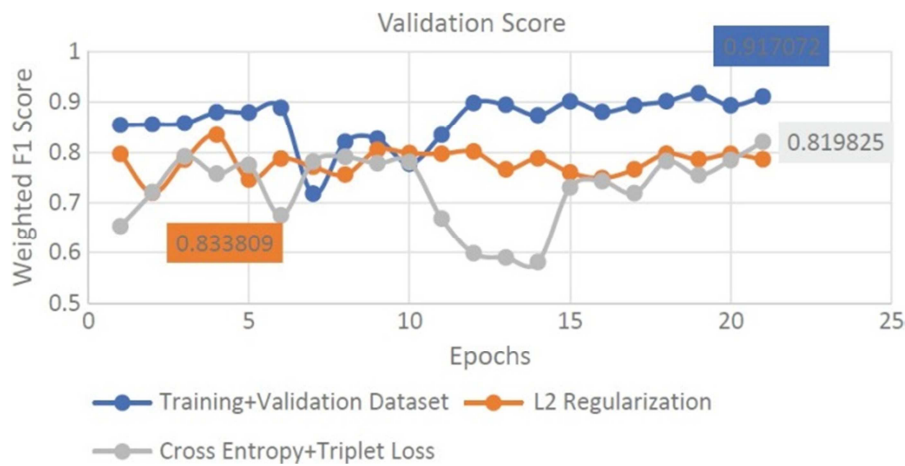


**Figure 7.** Using (i) A simple cross-entropy loss (training and validation dataset), (ii) fine-tuning the model to validate the set and weighted F1 fractional cross-entropy plus the three-state loss over time, combined with L2 normalized cross-entropy loss (0.001) and (iii). By marking the appropriate data points, you can indicate the best score. Fine-tune the combination of training and validation datasets used in Phase 1 to the network.

## 7. Experimental Results

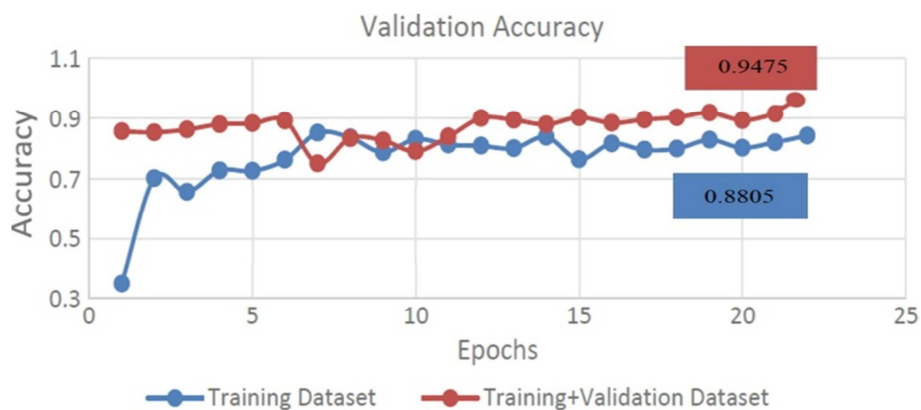


**Figure 8.** Check the model set's accuracy relative to the duration for fine-tuning models that use I training datasets and (ii) combined training and validation datasets for cross-entropy loss. The highest accuracy of each method is represented by marking the appropriate data points.

**Table 2.** Scores for test datasets.

Dataset	Weighted Precision	Weighted Recall	Weighted-F1 Score
Results	0.9470	0.9475	0.9470

## 8. Conclusions

Transfer learning and fine-tuning of the VGG16 convolutional neural network through batch normalization can resolve the malignant and normal white blood cells classification problem with higher accuracy. Applying CLAHE to enhance image data quality is then passed as input to the network for training purposes. The results acquired by the fine-tuning of triple-loss and cross-entropy or cross-entropy loss with L2 normalization are compared. Furthermore, fine-tuning on a combined training validation dataset using simple cross-entropy loss can improve the model's performance. The VGG16 network has some drawbacks because of the many layers and too many training parameters, making the model training process time-efficient. For achieving efficiency along with accuracy, some lightweight state-of-the-art deep learning models can also be considered.

The proposed model achieves an average accuracy of 94.75 for classifying malignant and normal cells, the higher accuracy obtained by the proposed model shows the effectiveness of transfer learning in cancer detection.

## References

- [1] N. Thanh, K. AL-Dulaimi, J. Banks, V. Chandran, I. Tomeo-Reyes, and K. Nguyen, "Classification of White Blood Cell Types from Microscope Images: Techniques and Challenges," pp. 17–25, 2018.
- [2] I. Mehmood et al., "An efficient computerized decision support system for the analysis and 3D visualization of brain tumor," *Multimed. Tools Appl.*, pp. 1–26, 2018.
- [3] A. Nedra, M. Shoaib, and S. Gattoufi, "Detection and classification of the breast abnormalities in Digital Mammograms via Linear Support Vector Machine," *Middle East Conf. Biomed. Eng. MECBME*, vol. 2018– March, pp. 141–146, 2018.
- [4] K. Kourou, T. P. Exarchos, K. P. Exarchos, M. V. Karamouzis, and D. I. Fotiadis, "Machine learning applications in cancer prognosis and prediction," *Comput. Struct. Biotechnol. J.*, vol. 13, pp. 8–17, 2015.
- [5] C. E. Condrat et al., "miRNAs as Biomarkers in Disease: Latest Findings Regarding Their Role in Diagnosis and Prognosis," *Cells*, vol. 9, no. 2, p. 276, 2020.
- [6] N. Bibi, M. Sikandar, I. U. Din, A. Almogren, and S. Ali, "IOMT-based automated detection and classification of leukemia using deep learning," *J. Healthc. Eng.*, vol. 2020, 2020.
- [7] W. Ladines-Castro et al., "Morphology of leukaemias," *Rev. Médica del Hosp. Gen. México*, vol. 79, no. 2, pp. 107–113, 2016.
- [8] A. R. M. Al-shamasneh and U. H. B. Obaidallah, "Artificial Intelligence Techniques for Cancer Detection and Classification: Review Study," *Eur. Sci. J.*, vol. 13, no. 3, pp. 342–370, 2017.
- [9] P. Szymak, P. Piskur, and K. Naus, "The effectiveness of using a pretrained deep learning neural networks for object classification in underwater video," *Remote Sens.*, vol. 12, no. 18, pp. 1–19, 2020.
- [10] G. Ayana, K. Dese, and S. Choe, "Transfer Learning in Breast Cancer Diagnoses via Ultrasound Imaging," 2021.
- [11] A. Luque-Chang, E. Cuevas, F. Fausto, D. Zaldívar, and M. Pérez, "Social Spider Optimization Algorithm: Modifications, Applications, and Perspectives," *Math. Probl. Eng.*, vol. 2018, 2018.
- [12] A. T. Sahlol, P. Kollmannsberger, and A. A. Ewees, "Efficient Classification of White Blood Cell Leukemia with Improved Swarm Optimization of Deep Features," *Sci. Rep.*, vol. 10, no. 1, pp. 1–11, 2020.
- [13] R. Aziz, C. K. Verma, and N. Srivastava, "Dimension reduction methods for microarray data: a review," *AIMS Bioeng.*, vol. 4, no. 1, pp. 179–197, 2017.
- [14] N. Ahmed, A. Yigit, Z. Isik, and A. Alpkocak, "Identification of leukemia subtypes from microscopic images using convolutional neural network," *Diagnostics*, vol. 9, no. 3, 2019.
- [15] S. Agrawal and J. Agrawal, "Neural network techniques for cancer prediction: A survey," *Procedia Comput. Sci.*, vol. 60, no. 1, pp. 769–774, 2015.
- [16] M. Adjouadi, M. Ayala, M. Cabrerizo, N. Zong, G. Lizarraga, and M. Rossman, "Classification of leukemia blood samples using neural networks," *Ann. Biomed. Eng.*, vol. 38, no. 4, pp. 1473–1482, 2010.
- [17] T. J. Sejnowski, "The unreasonable effectiveness of deep learning in artificial intelligence," *Proc. Natl. Acad. Sci.*, p. 201907373, 2020.
- [18] M. M. Amin, S. Kermani, A. Talebi, and M. G. Oghli, "Recognition of acute lymphoblastic leukemia cells in microscopic images using k-means clustering and support vector machine classifier," *J. Med. Signals Sens.*, vol. 5, no. 1, pp. 49–58, 2015.